Polym. Bull. (2012) 68:1731–1746
DOI 10.1007/s00289-011-0694-6

ORIGINAL PAPER

Photoinduced orientation and cooperative motion of three epoxy-based azo polymers

Yanwei Wang · Yaning He · Xiaogong Wang

Received: 29 September 2011 / Revised: 13 December 2011 / Accepted: 20 December 2011 /
Published online: 30 December 2011

Abstract In this work, photoinduced orientation of three epoxy-based polymers bearing different type azo chromophores was studied. The epoxy-based azo polymers were synthesized through post-polymerization azo-coupling reactions based on an epoxy-based precursor polymer (BP-AN), which was synthesized by the step polymerization between bisphenol-A diglycidyl ether and aniline. The chromophore orientation and cooperative motion of the main-chain groups were studied by birefringence characterization, polarized infrared spectroscopy, and two-dimensional (2D)-IR correlation spectroscopy (COS). The results show that the orientation behavior of the epoxy-based azo polymers is closely related with the electron-withdrawing groups on the azo chromophores. The azo polymer BP-AZ-CN, which contains azo chromophores with cyano as the electron-withdrawing group, shows the fastest birefringence growth rate. The azo polymer BP-AZ-CA, containing carboxyl as the electron-withdrawing group, possesses high birefringence residual value and the highest saturated orientation degree in the series. Cooperative motion between azobenzene moieties and non-photochromic polymer backbone was revealed by polarized FTIR and 2D-IR COS. The photoinduced anisotropy is a result of the orientation of both azo chromophore and polymer main-chain. The understanding of the structure–property relationships can be used to develop materials with better performance for data storage and other applications.

Keywords Azo polymer · Epoxy-based · Photoinduced orientation · Polarized FTIR · 2D-IR

Y. Wang · Y. He · X. Wang (✉)
Department of Chemical Engineering, Laboratory for Advanced Materials, Tsinghua University, Beijing 100084, People's Republic of China
e-mail: wxg-dce@mail.tsinghua.edu.cn

Introduction

Polymers containing azobenzene and its derivatives (azo polymers for short) have received considerable attention for their unique photoresponsive properties [1–10]. Among those properties, photoinduced molecular orientation is a property with special interest and has been intensively investigated for years [11–33]. The photoinduced orientation in polymer thin films can produce significant birefringence and dichroism, which are promising for applications in optical data storage, diffraction gratings, and other optical devices [11–13]. The mechanism of the photoinduced orientation involves the photochemical excitation of the azobenzene moieties [14, 15]. When irradiated with linearly polarized light, the azobenzene groups that are not perpendicular to the light polarization direction will undergo repeated *trans–cis–trans* isomerization. As a result, the azobenzene moieties will be forced to orientate in the direction perpendicular to the polarization of the incident light. In many cases, non-photochromic structures, such as the copolymerized side-chain groups, spacers, and polymer main-chain, can also be driven to align in a correlative direction due to the cooperative motion [16, 25–28]. The molecular orientation in the polymer films can be quantitatively characterized by the birefringence measurement, polarized UV–Vis spectroscopy, and polarized IR spectroscopy [14, 15, 24, 25]. In past decades, the correlation between the photoinduced orientation and molecular structures has been extensively studied for both liquid crystal azo polymers [12, 13, 29–33], and amorphous azo polymers [16–24]. Understanding of the structure–property relationships has been used to elucidate the mechanism and develop materials with better performance.

Epoxy-based azo polymers, which possess good thermal stability and transparency, have been studied for various photoresponsive properties [7, 34–42]. Typically, epoxy-based azo polymers are amorphous polymers constructed by bonding photoresponsive azo chromophores directly on the epoxy-based backbones through the amino linkage. Epoxy-based polymers containing different type azo chromophores have been used to fabricate the SRG and other surface patterns [7, 34, 35]. Epoxy-based azo polymers have been developed through post-polymerization azo-coupling scheme and studied as the non-linear optical materials [36–38]. Colloidal spheres composed of epoxy-based azo polymers have been prepared through self-assembling, which exhibit photoinduced deformation in the polarization direction of the incident laser [39–42]. Recently, photoinduced orientation in cross-linked epoxy-based azo polymers and guest–host systems has been investigated through birefringence measurements [43, 44]. However, most epoxy-based azo polymers mentioned above belong to the catalog of linear polymers without cross-linking. The linear epoxy-based azo polymers are also distinct from typical side-chain azo polymers as one end of the azo chromophores is directly tethered on the polymeric backbone without the flexible spacers. To our knowledge, the photoinduced orientation behavior of the linear epoxy-based azo polymers has not been systematically studied yet. It is still more or less unclear whether the azo chromophores can be driven by polarized light to take the predominant alignment as efficiently as side-chain azo polymers. Even less is known about the possible orientation correlation of the azo chromophore with other structural units of the polymers.

In this study, both birefringence measurement and FTIR spectroscopy were used to investigate the orientation in the epoxy-based azo polymer films, when they were irradiated with a linearly polarized Ar^+ laser beam. The three epoxy-based polymers bearing different type azo chromophores were used for the investigation. The photoinduced birefringence growth rate and saturated degree were measured to understand the orientation behavior. The polarized FTIR was used to provide the molecular level information of the orientation. Two-dimensional correlation spectroscopy (2D-COS) was applied to study the cooperative effect between the azo chromophores and polymer main-chain.

Experimental section

Materials

The epoxy-based azo polymers were prepared through post-polymerization azo-coupling scheme as reported previously [45]. The chemical structure of the epoxy-based azo polymers, BP-AZ-CN, BP-AZ-CA, and BP-AZ-NT, is given in Fig. 1. The epoxy-based precursor polymer (BP-AN) was obtained through the step polymerization between bisphenol-A diglycidyl ether (BADGE) and aniline. The azo polymers were prepared through azo-coupling reactions between BP-AN and diazonium salts of 4-aminobenzonitrile, 4-aminobenzoic acid, and 4-nitroaniline, respectively. The number-average molecular weight of BP-AN was 35,000 with a polydispersity index of 2.2. The degree of functionalization of BP-AZ-CN, BP-AZ-CA, and BP-AZ-NT was 100, 91, and 100%. The synthesis and characterization

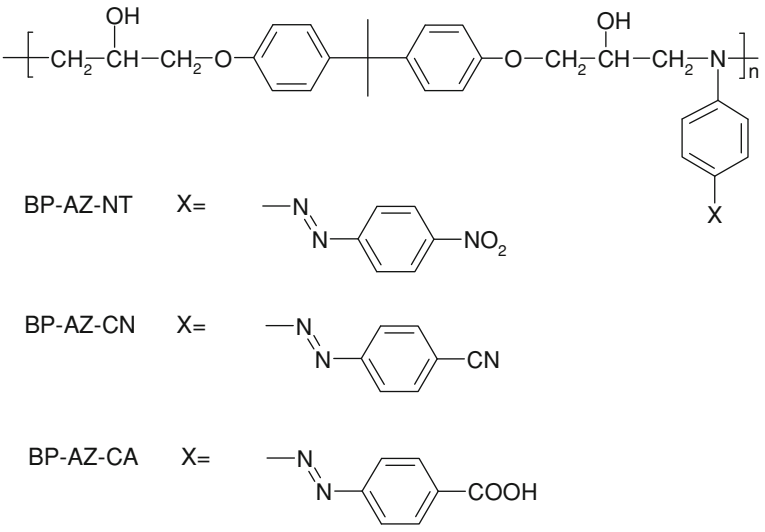

Fig. 1 Chemical structure of BP-AZ-NT, BP-AZ-CN, and BP-AZ-CA

details have been given in our previous paper [45]. All other materials and solvents were commercially available products, which were used as received without further purification.

Film preparation

Analytical pure *N*,*N*-dimethylformamide (DMF) was used as the solvent to dissolve the azo polymers. The epoxy-based azo polymers were dissolved in DMF with a concentration of 0.1 g/mL. After filtered through 0.45-μm membrane, the solutions were spin-coated onto clean glass slides or calcium fluoride (CaF_2) disks under the same condition. The film thickness was controlled to be about 400 nm by adjusting the spin speed. The spin-coated films were dried at 70 °C under vacuum for 48 h and stored in a desiccator for further measurements.

Birefringence measurement

The photoinduced orientation behavior of the epoxy-based azo polymers was studied through the birefringence measurement. The photoinduced birefringence of the films was obtained by the method described in previous literature [23–25]. A linearly polarized laser beam from an Ar^+ laser (488 nm) with the intensity of 50 mW/cm^2 was used as the light source. For the measurements, a piece of the azo-polymer films was placed between a pair of crossed polarizers, which were set up to be 45° with respect to the polarization angle of the incident laser beam. A lower power He–Ne laser at 632.8 nm was used to measure the transmitted power through optical setup. The angle between incident laser beam and probing laser beam was fixed to be 8°. The photoinduced birefringence of azo polymer film was monitored by the transmittance of probing laser beam until the signal reached the saturated state, and then the writing incident laser beam was turned off to investigate the birefringence relaxation process. The transmittance of probing laser beam normalized by the saturated value (I/I_0) was used to describe the photoinduced birefringence growth and decay processes. The I_0 is the intensity of the transmitted probing laser when the transmittance signal of probing laser beam reached the saturated state, and I is the transmittance recorded during the laser irradiating and dark relaxation processes. The growth and decay curves were obtained under the same condition for comparison. All experiments were carried out at room temperature under air-ambient condition.

Polarized FTIR

The photoinduced orientation was studied by polarized FTIR similar to the method described in previous literature [28, 46, 47]. The azo polymer films spin-coated on calcium fluoride disks were irradiated with the linearly polarized Ar^+ laser beam to induce the orientation under the same condition mentioned above for the birefringence characterization. Polarized infrared spectra of the samples were obtained at room temperature using a Nicolet 560-IR FTIR spectrometer equipped with a wire grid polarizer (KRS-5). In the measurements, the spectra from 32 scans

were collected with a resolution of 4 cm^{-1}. The dichroic ratio R is defined as $A_{\perp}/A_{\parallel}$, where $A_{\parallel}$ and $A_{\perp}$ are the absorbances in the parallel and perpendicular directions to the exciting laser polarization.

2D-FTIR calculations

Synchronous and asynchronous correlation spectra were calculated based on the principles proposed by Noda [48] using the software package developed with Matlab 6.5. The dynamic spectrum $\tilde{A}(v,t)$ is defined as

$$\tilde{A}(v,t) = A(v,t) - \bar{A}(v) \tag{1}$$

where $\bar{A}(v)$ is the average spectrum as the reference spectrum, and $A(v,t)$ is the spectrum after the film irradiated for time t. In this study, $A(v,t)$ is recorded at the angle 45° between the polarization directions of polarized infrared radiation and polarized exciting laser [48, 49]. The cross-spectrum $X(v_1, v_2)$ between the intensities of dynamic spectrum measured at two different wavenumbers is given by

$$\begin{aligned} X(v_1, v_2) &= \frac{<\tilde{A}(v_1,t) \cdot \tilde{A}(v_2,t)>}{2T} \\ &= \Phi(v_1, v_2) - i\psi(v_1, v_2) \end{aligned} \tag{2}$$

where $\Phi(v_1, v_2)$ and $\Psi(v_1, v_2)$ represent the individual Fourier component of the synchronous and asynchronous 2D correlation spectrum, respectively. In this study, the contour maps are constructed from synchronous and asynchronous 2D correlation spectrum based on the process proposed by Noda [48].

Results and discussion

The chemical structure of the epoxy-based azo polymers used for the study is given in Fig. 1. The azo polymers were prepared through the post-polymerization azo-coupling reactions between the precursor polymer (BP-AN) and the corresponding diazonium salts [45]. The main difference between the polymers is the azo chromophores bearing the different electron-withdrawing groups. Figure 2 give the UV–Vis spectra of the azo polymers in DMF solutions. The λ_{max}s of the π–π^* transition of the polymers in DMF solutions and as spin-coated films are given in Table 1. The degree of functionalization of BP-AZ-CN, BP-AZ-CA, and BP-AZ-NT is 100, 91, and 100% determined by ^{1}H NMR spectroscopy. As the same-batch of the precursor polymer is used in the post-functionalization reactions, the degree of polymerizations (DP) of the azo polymers are same, which can avoid possible influence of DP on the properties in the following study. The synthesis and characterization details of the polymers can be seen in our previous article [45]. The solid thin films of the azo polymers were obtained by spin-coating. The molecular orientation in the azo polymer films was induced by the irradiation with a linearly polarized Ar^+ laser beam (488 nm). The results obtained from the birefringence

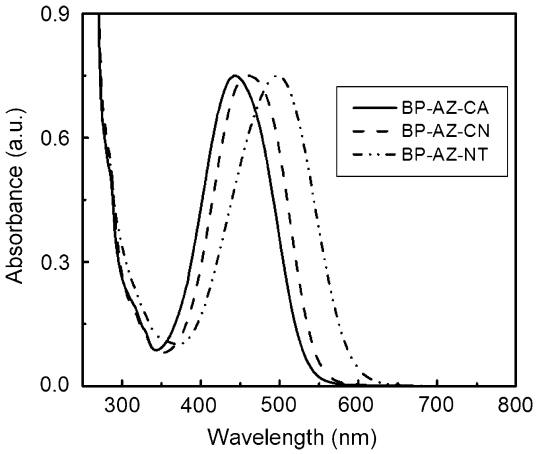

Fig. 2 The UV–Vis spectra of the azo polymers in DMF solution

Table 1 λ_{max}s of the azo polymers in DMF solution and as spin-coated films

Azo polymer	λ_{max} (nm) (in DMF solution)	λ_{max} (nm) (as spin-coated films)
BP-AZ-NT	498	482
BP-AZ-CN	460	449
BP-AZ-CA	445	431

measurements, polarized FTIR spectroscopy, 2D-FTIR investigation are presented as follows.

Photoinduced birefringence

The photoinduced birefringence measurement was used to investigate the molecular orientation upon the polarized laser irradiation. For the measurements, spin-coated films of BP-AZ-CN, BP-AZ-CA, and BP-AZ-NT on glass slides were exposed to a linearly polarized Ar^+ laser beam (488 nm, 50 mW/cm^2). The birefringence variations during the light irradiation and relaxation processes were recorded in a real-time manner. Figure 3 shows the growth and decay curves of the reduced transmittance (I/I_0) of spin-coated films for BP-AZ-NT, BP-AZ-CN, and BP-AZ-CA, where I and I_0 are the transmittances at time t and saturated states. Before irradiation, no transmission of the probing beam through the crossed polarizer is observed, which indicates that the azo polymer films are homogeneous and optically isotropic. When the polymer films are irradiated, the transmittance of probing beam increases gradually due to the optical anisotropy induced in the polymer films. When the incident laser beam is turned off, the transmission of probing beam decreases quickly, corresponding to the partial relaxation of the photoinduced anisotropy in the polymer films. The transmittance variation reflects birefringence change corresponding to the molecular orientation and relaxation in the polymer films. As it can be seen in Fig. 3, the birefringence growth rate and residual value after the relaxation are closely related to the structure of azo chromophores. The

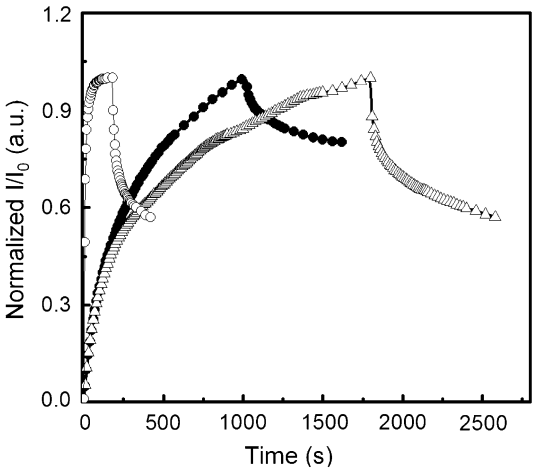

Fig. 3 Growth and decay curves of photoinduced birefringence in films of BP-AZ-NT (*open triangle*), BP-AZ-CN (*open circle*), and BP-AZ-CA (*filled circle*), respectively

birefringence of BP-AZ-CN film reaches the maximum value in the shortest time but quickly relaxes after switching off the light. The birefringence growth of BP-AZ-NT is the slowest in the series. BP-AZ-CA shows an intermediate growth rate and the largest birefringence residual value after the relaxation compared with the other two polymers.

The transmittance (I/I_0) growth and decay curves can be best fitted by a biexponential function as below:

$$y = A(1 - \exp(-k_a t)) + B(1 - \exp(-k_b t)) \quad (3)$$

$$y = C\exp(-k_c t) + D\exp(-k_d t) + E \quad (4)$$

where y is the transmittance of probing beam, k_a and k_b are the growth rate constants for fast and slow processes, while k_c and k_d are the relaxation rate constants for fast and slow processes; the parameters; A, B, C, and D are the relative contributions of the processes; and E represents the residual birefringence in the film after the relaxation [18, 24, 32, 50]. The fitted parameters obtained by using Eqs. 3 and 4 are listed in Table 2, where the coefficients of determination (R^2) are all larger than 0.996. Previous studies have indicated that the fast and slow modes are related to the dynamic processes of the azobenzene moiety and polymeric chain, respectively [18, 26]. The result shows that BP-AZ-CN possesses the largest birefringence growth rates and relaxation rates for both fast and slow processes. BP-AZ-NT and BP-AZ-CA have the similar birefringence growth rate for the fast processes. But, because of the larger k_b (the slow process), BP-AZ-CA shows the faster birefringence growth rate compared with BP-AZ-NT. BP-AZ-CA shows the smallest relaxation rates, especially for the slow process, and largest residual value after the relaxation ($E = 0.791$).

Hydrogen bonding characterization

Above results indicate that the three epoxy-based azo polymers show significantly difference in the photoinduced birefringence behavior. Since the photoinduced

Table 2 Fitted parameters obtained from the reduced transmittance (I/I_0) growth and decay curves of BP-AZ-CN, BP-AZ-CA, and BP-AZ-NT

	k_a (s^{-1})	k_b (s^{-1})	k_c (s^{-1})	k_d (s^{-1})	A_n[a]	B_n[a]	C_n[b]	D_n[b]	E
BP-AZ-CN	0.211	0.043	0.104	0.010	0.645	0.355	0.523	0.477	0.501
BP-AZ-CA	0.013	0.002	0.050	0.004	0.275	0.725	0.315	0.685	0.791
BP-AZ-NT	0.014	0.001	0.077	0.003	0.331	0.669	0.388	0.612	0.546

[a] $A_n = A/(A + B)$, $B_n = B/(A + B)$

[b] $C_n = C/(C + D)$, $D_n = D/(C + D)$

birefringence of azo polymer film is correlated with the motion of both azo chromophores and polymer segments, the molecular interaction through hydrogen bonding could play an important role in the process. To clarify this issue, infrared spectroscopy was conducted to study the hydrogen bonding of the epoxy-based azo polymers. Figure 4a presents the infrared spectra in 3,100–3,750 cm^{-1} region of the azo polymers before irradiation, where the bands belong to O–H stretching vibration. It can be seen that the absorption bands of these three polymers are very broad and these absorption bands shift to the lower frequency from the normal O–H stretching vibration band position (3,600 cm^{-1}), which is more significant for BP-AZ-NT. It indicates that the hydrogen bonding exists in samples, especially for BP-AZ-NT. For BP-AZ-CA, the hydrogen bonding also exists for the COOH groups on the azo chromophores as confirmed by the lower frequency of the stretching vibration of C=O (Fig. 4b). As the motion of both azo chromophores and polymer main-chain are restricted by the hydrogen bonding, BP-AZ-CA shows the slower birefringence growth rate compared with BP-AZ-CN. The high residual birefringence of BP-AZ-CA could also be attributed to the restriction of the hydrogen bonding to the relaxation. For BP-AZ-NT, the strong hydrogen bonding can be one of the factors that cause the slower orientation of the azo chromophores. Other possible influences will be given in the "Discussion" section.

Polarized FTIR

The polarized FTIR spectroscopy was applied to investigate the molecular orientation of the azo polymers. For the measurements, spin-coated films of BP-AZ-CN, BP-AZ-CA, and BP-AZ-NT on CaF_2 disks were irradiated with a linearly polarized laser beam (488 nm, 50 mW/cm^2) until the birefringence reached the saturated value. The polarized infrared spectra were collected in two directions, where the polarized infrared light is perpendicular ($A_\perp$) and parallel ($A_\parallel$) to the exciting laser polarization, respectively. Figure 5 shows the IR spectra together with the difference spectra ($\Delta A = A_\perp - A_\parallel$). The assignments and the structure origin of the characteristic absorption bands in these spectra are summarized in Table 3. As shown in Fig. 5, the positive differences exist for the characteristic vibrations in the spectral region, which indicates that both azobenzene moieties and related main-chain groups prefer to orientate perpendicular to the polarization of the exciting light.

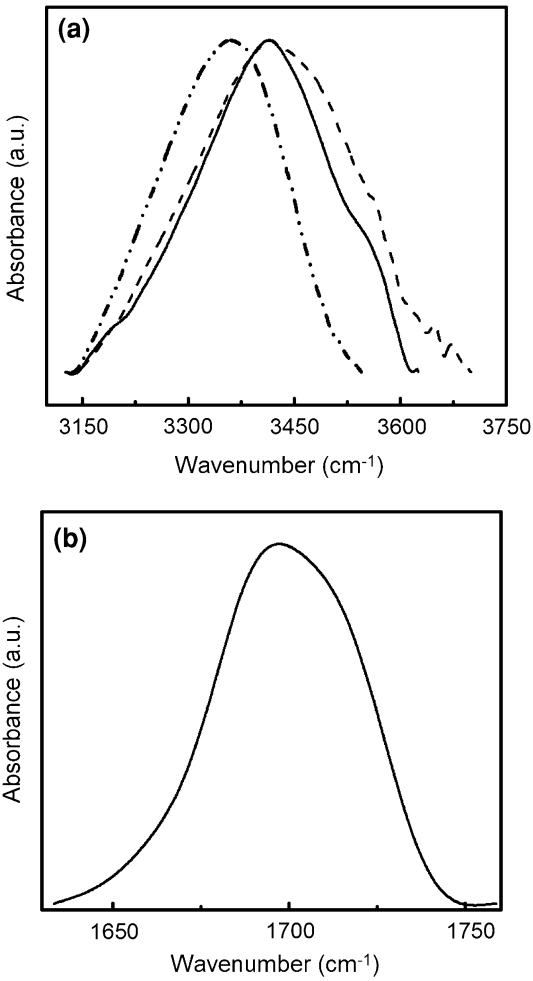

Fig. 4 **a** Infrared spectra associated with O–H stretching vibration of BP-AZ-CA (*continuous line*), BP-AZ-CN (*dashed line*), and BP-AZ-NT (*dashed dotted line*); **b** Infrared spectrum of C=O stretching vibration of BP-AZ-CA

To further understand the orientation of the azobenzene moieties and main-chain groups, the polarized FTIR spectra were measured when the polarized infrared light direction changed from 0° to 180° with 5° interval for these three epoxy-based azo polymers. The bands of the ν(N=N) and ν_{as}(C–O–Ar) vibrations, associated with the azo chromophores and the ether linkages of the main-chains, respectively, are presented here. The vibrations associated with these bands have their transition dipole moment parallel to the long axis of the azobenzene and phenyl groups [25, 27]. As the absorption bands are well resolved, they can be used as the molecular probes to study the orientation behavior of the azobenzene moieties and the bisphenol-A moieties of the backbone. Figure 6 presents polar diagrams for absorbance of ν(N=N) and ν_{as}(C–O–Ar) vibrations of BP-AZ-CN, BP-AZ-CA, and BP-AZ-NT. In the figures, the normalized absorbance of these two bands is plotted as a function of rotational angle (α) between the polarization directions of the

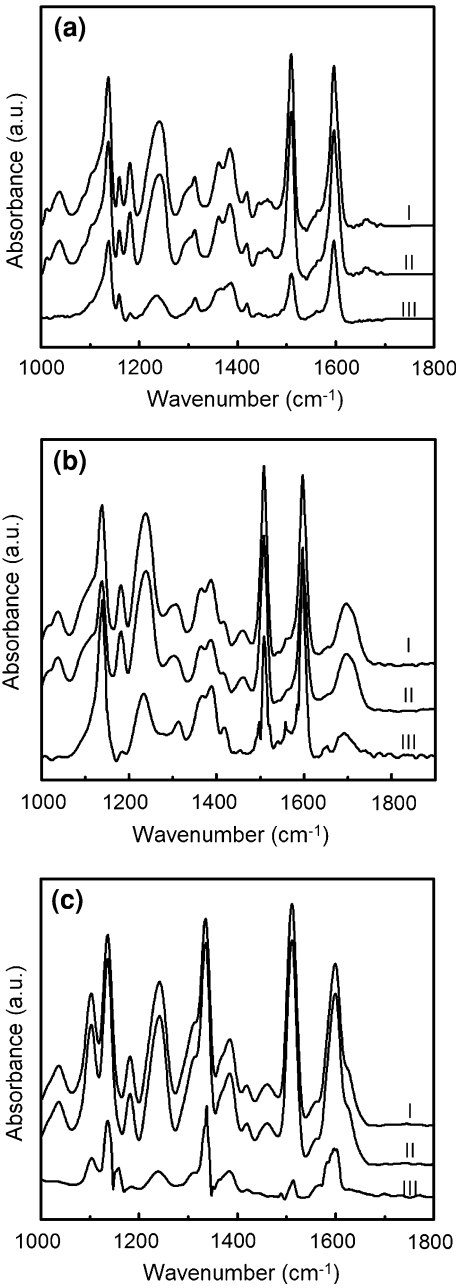

Fig. 5 Polarized FTIR spectra of **a** BP-AZ-CN, **b** BP-AZ-CA, and **c** BP-AZ-NT after irradiation with 488 nm linear polarized laser. (*I*) $A_{\perp}$, (*II*) $A_{\parallel}$, and (*III*) $\Delta A = A_{\perp} - A_{\parallel}$

exciting laser and the infrared light. The absorbance (A) was normalized by the corresponding absorbance $A_{\parallel}$ from the same vibration and $A/A_{\parallel}$ represents the dichroic ratio (R) when $\alpha = 90°$ and 270°. The result reveals that the azobenzene moieties show predominant orientation in the directions perpendicular to the

Table 3 Assignment, frequency, and structure origin of the characteristic bands in the infrared spectra of azo polymers under consideration

Assignment	Frequency (cm^{-1})			Structure origin
	BP-AZ-CN	BP-AZ-CA	BP-AZ-NT	
ν_s(CN)	2,227			Azo chromophore
ν(C=O)		1,699		Azo chromophore
ν(C=C)$_{Ar}$	1,596/1,509	1,597/1,508	1,599/1,511[a]	Benzene ring
ν_{as}(NO_2)			1,511[a]	Azo chromophore
ν(N=N)	1,385	1,387	1,385	Azo chromophore
ν_s(NO_2)			1,336	Azo chromophore
ν_{as}(C–O–Ar)	1,247	1,238	1,241	Bisphenol-A moieties
ν_s(=N–Ar)	1,136	1,138	1,136	Azo chromophore

as asymmetric, *s* symmetric, *Ar* aromatic

[a] Overlapped band of ν(C=C)$_{Ar}$ and ν_{as}(NO_2)

polarization of the excitation laser beam. It confirms that the birefringence observed above is mainly caused by the chromophore orientation. The orientation degree of BP-AZ-CA is much larger than those of BP-AZ-CN and BP-AZ-NT. The ether linkages of the bisphenol-A moieties of the backbone also show the correlative orientation induced by the light irradiation although the orientation degrees are smaller than those of the azo chromophores. For the azo polymers, the orientation degree of the ether linkage in BP-AZ-CA backbone is much larger than that of BP-AZ-CN and BP-AZ-NT. It reveals the existence of the cooperative motion between the orientation of the azo chromophores and polymer main-chain groups.

2D-COS investigation

The 2D-FTIR COS was used to investigate the time dependent orientation process when the azo polymer films were irradiated by the linearly polarized laser. As a typical case, the BP-AZ-CN film spin-coated on CaF_2 disk was irradiated by the same exciting laser (488 nm, 50 mW/cm^2) for different time, 10, 20, 30, 40, 50, and 60 s. Figure 7 shows the synchronous and asynchronous contour maps calculated from the dynamic spectra in the region 1,050–1,450 cm^{-1}. The contour maps were obtained based on the principle presented in "Experimental section" and previous literature [48].

In Fig. 7a, all the cross-peaks are positive, showing that the intensity of the bands related to the groups of main-chain and azo chromophores changes in the same direction. It indicates that the orientation directions of both azo chromophore and the groups of main-chain are same when BP-AZ-CN is irradiated by linearly polarized laser beam. And the positive cross-peaks observed between the band at 1,247 cm^{-1} (ν_{as}(C–O–Ar)) and the bands at 1,137 cm^{-1} (ν_s(=N–Ar)), and 1,385 cm^{-1} (ν(N=N)) further confirm that the ether linkage of the main-chain and the azo chromophores has a significant cooperative motion during their orientation process, which is consistent with the conclusion drawn from polarized FTIR

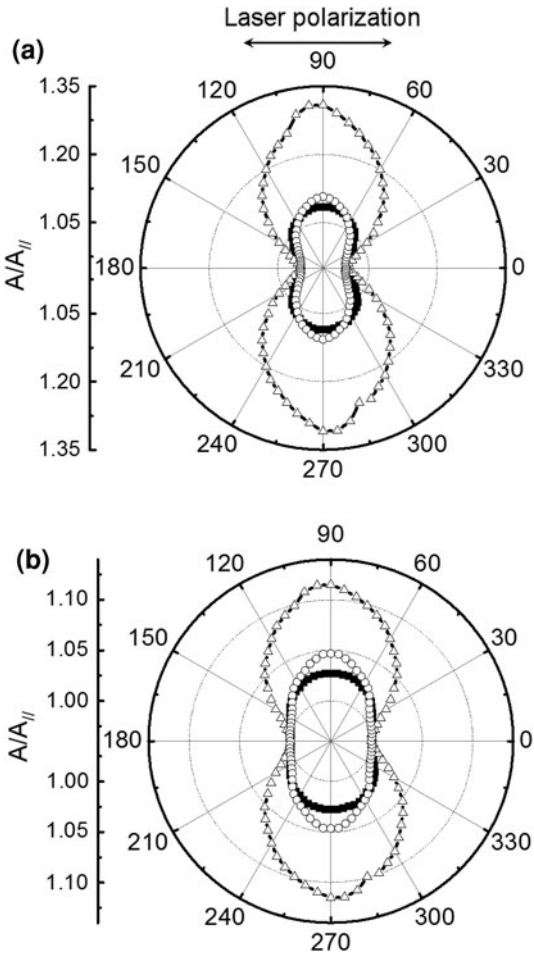

Fig. 6 Polar plots of the normalized absorbance as a function of rotational angle (α) for **a** ν(N=N) and **b** ν_{as}(C–O–Ar) of BP-AZ-CN (*open circle*), BP-AZ-CA (*open triangle*), and BP-AZ-NT (*filled square*)

analysis. While in the asynchronous contour map (Fig. 7b), a positive cross-peak is observed at 1,247–1,385 cm^{-1}. According to the principle proposed by Noda [48], these results indicate that the orientation of the main-chain groups is somehow faster than that of azo chromophore. This result suggests that the orientation of the main-chain induced by the first *trans–cis–trans* isomerization cycles of the azobenzene groups can be preserved during the rest of the orientation process. This observation is similar to the previous conclusion from the orientation study of a semi-crystalline polymer [49].

Discussion

The results obtained above show that the electron-withdrawing groups on the azo chromophores significantly affect the photoinduced orientation behavior of the epoxy-based azo polymers. The influence can be rationalized by considering the isomerization

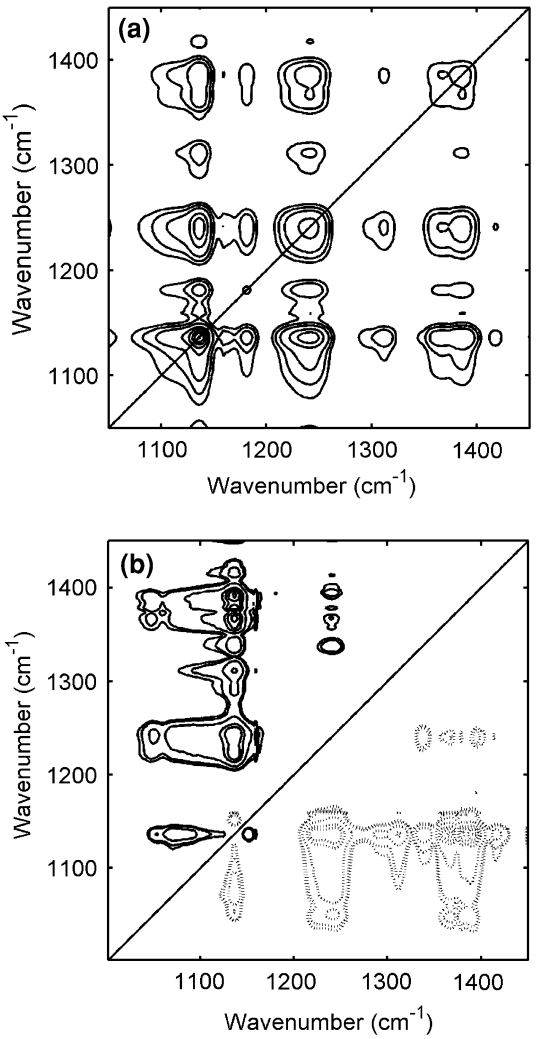

Fig. 7 **a** Synchronous and **b** asynchronous contour maps of BP-AZ-CN irradiated for different time periods. The *solid* and *dotted lines* represent positive and negative peaks, respectively

efficiency of the azo chromophores and intermolecular interaction through hydrogen bonding. The *trans–cis* photoisomerization efficiency is dependent on the competition between excitation (π–π^* or n–π^* transition) and relaxation [51]. The *trans–cis* isomerization yield of the n–π^* excitation is higher than that of the π–π^* excitation. As the λ_{max} of the n–π^* excitation of BP-AZ-CN is close to the excitation wavelength (488 nm), the largest birefringence growth rate can be attributed to the higher isomerization efficiency. For BP-AZ-CA, the situation can be more complicated. On one hand, the n–π^* transition band is also close to the excitation wavelength, which can cause efficient *trans–cis* isomerization. One the other hand, as the hydrogen bonding of the COOH groups exists in the polymer, it inhibits the chromophore motion and results in the slower birefringence growth rate compared with BP-AZ-CN. The higher birefringence residual value after relaxation can also be attributed to the hydrogen bonding, which restricts the motion of

the oriented azo chromophores. Therefore, the orientation degree of BP-AZ-CA measured by IR spectroscopy is much larger than those of BP-AZ-CN and BP-AZ-NT. As the hydrogen bonding is relatively weak in BP-AZ-CN, the photoinduced birefringence quickly relax when switching off the light. For BP-AZ-NT, the excitation wavelength is closer to the π–π^* transition band in addition to the factor that there exists strong hydrogen bonding in the system. Therefore, it shows the slowest birefringence growth rate and the lowest orientation degree of the azo chromophores.

Conclusion

The photoinduced orientation behavior of three epoxy-based azo polymers, BP-AZ-CN, BP-AZ-CA, and BP-AZ-NT, was investigated by using the birefringence measurement, polarized FTIR, and 2D-IR COS. Although one end of the azo chromophores is tethered on the polymer main-chains, the chromophores can be efficiently driven by polarized light to take the orientation perpendicular to the polarization of the exciting light. The orientation behavior is closely related to the electron-withdrawing groups on the azo chromophores. Among the polymers, BP-AZ-CN containing the cyano group on the azo chromophore shows the fastest birefringence growth rate, while BP-AZ-CA containing the carboxyl group shows the highest birefringence residual value. The polymer backbone shows a cooperative motion with the azo chromophore during the photoinduced orientation process. The results from 2D-IR COS further confirm that the polymer main-chain and azo chromophore have a strong cooperative motion during the photoinduced orientation process. The hydrogen bonding between the COOH groups of BP-AZ-CA can play an important role to influence the photoinduced orientation and relaxation behavior. Due to this reason, BP-AZ-CA shows the highest saturated orientation degrees for both azo chromophore and correlated main-chain groups.

Acknowledgment Financial support from the NSFC under projects 91027024 and 51061130556 is gratefully acknowledged.

References

1. Xie S, Natansohn A, Rochon P (1993) Recent developments in aromatic azo polymers research. Chem Mater 5(4):403–411
2. Delaire JA, Nakatani K (2000) Linear and nonlinear optical properties of photochromic molecules and materials. Chem Rev 100(5):1817–1845
3. Natansohn A, Rochon P (2002) Photoinduced motions in azo-containing polymers. Chem Rev 102(11):4139–4175
4. Ikeda T, Mamiya J, Yu YL (2007) Photomechanics of liquid-crystalline elastomers and other polymers. Angew Chem Int Ed 46:506–528
5. Ikeda T, Horiuchi S, Karanjit DB, Kurihara S, Tazuke S (1990) Photochemically induced isothermal phase transition in polymer liquid crystals with mesogenic phenyl benzoate side chains. 2. photochemically induced isothermal phase transition behaviors. Macromolecules 23:42–48
6. Rochon P, Batalla E, Natansohn A (1995) Optically induced surface gratings on azoaromatic polymer-films. Appl Phys Lett 66(2):136–138
7. Kim DY, Tripathy SK, Li L, Kumar J (1995) Laser-induced holographic surface-relief gratings on nonlinear-optical polymer-films. Appl Phys Lett 66(10):1166–1168

8. Li MH, Keller P, Li B, Wang XG, Brunet M (2003) Light-driven side-on nematic elastomer actuators. Adv Mater 15(7–8):569–572
9. Yu YL, Nakano M, Ikeda T (2003) Directed bending of a polymer film by light - Miniaturizing a simple photomechanical system could expand its range of applications. Nature 425(6954):145
10. Camacho-Lopez M, Finkelmann H, Palffy-Muhoray P, Shelley M (2004) Fast liquid-crystal elastomer swims into the dark. Nat Mater 3:307–310
11. Todorov T, Nikolova L, Tomova N (1984) Polarization holography.1. A new high-efficiency organic material with reversible photoinduced birefringence. Appl Optics 23(23):4309–4312
12. Eich M, Wendorff J, Reck B (1987) Reversible digital and holographic optical storage in polymeric liquid-crystals. Makromoleculare Chemie 8:59–63
13. Eich M, Wendorff J (1990) Laser-induced gratings and spectroscopy in monodomains of liquid-crystalline polymers. J Opt Soc Am B 7(8):1428–1436
14. Natansohn A, Rochon P, Gosselin J, Xie S (1992) Azo polymers for reversible optical storage. 1. Poly[4′-[[2-(acryloyloxy)ethyl]ethylamino]-4-nitroazobenzene]. Macromolecules 25(8):2268–2273
15. Natansohn A, Xie S, Rochon P (1992) Azo polymers for reversible optical storage. 2. Poly[4′-[[2-(acryloyloxy)ethyl]ethylamino]-2-chloro-4-nitroazobenzene]. Macromolecules 25(20):5531–5532
16. Natansohn A, Rochon P, Pezolet M, Audet P, Brown D, To S (1994) Azo polymers for reversible optical storage. 4 Cooperative motion of rigid groups in semicrystalline polymers. Macromolecules 27(9):2580–2585
17. Brown D, Natansohn A, Rochon P (1995) Azo polymers for reversible optical storage. 5 Orientation and dipolar interactions of azobenzene side-groups in copolymers and blends containing methylmethacrylate structural units. Macromolecules 28(18):6116–6123
18. Ho MS, Natansohn A, Rochon P (1995) Azo polymers for reversible optical storage. 7 The effect of the size of the photochromic groups. Macromolecules 28(18):6124–6127
19. Natansohn A, Rochon P, Ho MS, Barrett C (1995) Azo polymers for reversible optical storage. 6. Poly[4-[2-(methacryloyloxy)ethyl]azobenzene]. Macromolecules 28(12):4179–4183
20. Ho MS, Natansohn A, Rochon P (1996) Azo polymers for reversible optical storage. 9 Copolymers containing two types of azobenzene side groups. Macromolecules 29(1):44–49
21. Meng X, Natansohn A, Barrett C, Rochon P (1996) Azo polymers for reversible optical storage. 10 Cooperative motion of polar side groups in amorphous polymers. Macromolecules 29(3):946–952
22. Meng X, Natansohn A, Rochon P (1996) Azo polymers for reversible optical storage. 11. Poly{4,4′-(1-methylethylidene)bisphenylene 3-[4-(4-nitrophenylazo)Phenyl]-3-aza-pentanedioate}. J Polym Sci Pol Phys 34(8):1461–1466
23. Meng X, Natansohn A, Rochon P (1997) Azo polymers for reversible optical storage. 13 Photo-orientation of rigid side groups containing two azo bonds. Polymer 38(11):2677–2682
24. Song OK, Wang CH, Pauley MA (1997) Dynamic processes of optically induced birefringence of azo compounds in amorphous polymers below T-g. Macromolecules 30(22):6913–6919
25. Buffeteau T, Natansohn A, Rochon P, Pezolet M (1996) Study of cooperative side group motions in amorphous polymers by time dependent infrared spectroscopy. Macromolecules 29(27):8783–8790
26. Stumpe J, Lasker L, Fischer T, Rutloh M, Kostromin S, Ruhmann R (1996) Photo-orientation in amorphous and aligned films of photochromic liquid crystalline polymers. Thin Solid Films 285:252–256
27. Natansohn A, Rochon P, Meng XS, Barrett C, Buffeteau T, Bonenfant S, Pezolet M (1998) Molecular addressing? Selective photoinduced cooperative motion of polar ester groups in copolymers containing azobenzene groups. Macromolecules 31(4):1155–1161
28. Kulinna C, Hvilsted S, Hendann C, Siesler HW, Ramanujam PS (1998) Selectively deuterated liquid crystalline cyanoazobenzene side-chain polyesters. 3 Investigations of laser-induced segmental mobility by Fourier transform infrared spectroscopy. Macromolecules 31(7):2141–2151
29. Ishiguro M, Sato D, Shishido A, Ikeda T (2007) Bragg-type polarization gratings formed in thick polymer films containing azobenzene and tolane moieties. Langmuir 23(1):332–338
30. Wu YL, Demachi Y, Tsutsumi O, Kanazawa A, Shiono T, Ikeda T (1998) Photoinduced alignment of polymer liquid crystals containing azobenzene moieties in the side chain. 2. Effect of spacer length of the azobenzene unit on alignment behavior. Macromolecules 31(4):1104–1108
31. Wu YL, Zhang QJ, Kanazawa A, Shiono T, Ikeda T, Nagase Y (1999) Photoinduced alignment of polymer liquid crystals containing azobenzene moieties in the side chain. 5 Effect of the azo contents on alignment behavior and enhanced response. Macromolecules 32(12):3951–3956

32. Wu YL, Kanazawa A, Shiono T, Ikeda T, Zhang QJ (1999) Photoinduced alignment of polymer liquid crystals containing azobenzene moieties in the side chain. 4 Dynamic study of the alignment process. Polymer 40(17):4787–4793
33. Han DH, Tong X, Zhao Y, Galstian T, Zhao Y (2010) Cyclic azobenzene-containing side-chain liquid crystalline polymers: synthesis and topological effect on mesophase transition, order, and photoinduced birefringence. Macromolecules 43(8):3664–3671
34. Wang XG, Balasubramanian S, Kumar J, Tripathy SK, Li L (1998) Azochromophore-functionalized polyelectrolytes. 1 Synthesis, characterization, and photoprocessing. Chem Mater 10(6):1546–1553
35. Kim MJ, Kumar J, Kim DY (2003) Photofabrication of superhelix-like patterns on azobenzene polymer films. Adv Mater 15(23):2005–2008
36. Wang XG, Chen JI, Marturunkakul S, Li L, Kumar J, Tripathy SK (1997) Epoxy-based nonlinear optical polymers functionalized with tricyanovinyl chromophores. Chem Mater 9(1):45–50
37. Wang XG, Kumar J, Tripathy SK, Li L, Chen JI, Marturunkakul S (1997) Epoxy-based nonlinear optical polymers from post azo coupling reaction. Macromolecules 30(2):219–225
38. Wang XG, Yang K, Kumar J, Tripathy SK, Chittibabu KG, Li L, Lindsay G (1998) Heteroaromatic chromophore functionalized epoxy-based nonlinear optical polymers. Macromolecules 31(13): 4126–4134
39. Li YB, He YN, Tong XL, Wang XG (2005) Photoinduced deformation of amphiphilic azo polymer colloidal spheres. J Am Chem Soc 127(8):2402–2403
40. Li YB, He YN, Tong XL, Wang XG (2006) Stretching effect of linearly polarized Ar + laser single-beam on azo polymer colloidal spheres. Langmuir 22(5):2288–2291
41. Liu JP, He YN, Wang XG (2009) Size-dependent light-driven effect observed for azo polymer colloidal spheres with different average diameters. Langmuir 25(10):5974–5979
42. Liu JP, He YN, Wang XG (2008) Azo polymer colloidal spheres containing different amounts of functional groups and their photoinduced deformation behavior. Langmuir 24(3):678–682
43. Fernandez R, Mondragon I, Galante MJ, Oyanguren PA (2009) Bonding and molecular environment effects on photoorientation in epoxy-based polymers having azobenzene units. Eur Polym J 45(3): 788–794
44. Fernandez R, Mondragon I, Galante M, Oyanguren P (2009) Influence of chromophore concentration and network structure on the photo-orientation properties of crosslinked epoxy-based azopolymers. J Polym Sci Pol Phys 47(10):1004–1014
45. He YN, Wang XG, Zhou QX (2002) Epoxy-based azo polymers: synthesis, characterization and photoinduced surface-relief-gratings. Polymer 43(26):7325–7333
46. Tawa K, Kamada K, Kiyohara K, Ohta K, Yasumatsu D, Sekkat Z, Kawata S (2001) Photoinduced reorientation of azo dyes bonded to polyurethane studied by polarized FT-IR spectroscopy. Macromolecules 34(23):8232–8238
47. Han M, Kidowaki M, Ichimura K, Ramanujam PS, Hvilsted S (2001) Influence of structures of polymer backbones on cooperative photoreorientation behavior of *p*-cyanoazobenzene side chains. Macromolecules 34(12):4256–4262
48. Noda I (1993) Generalized 2-dimensional correlation method applicable to infrared, raman, and other types of spectroscopy. Appl Spectrosc 47(9):1329–1336
49. Buffeteau T, Pezolet M (1998) Photoinduced orientation in azopolymers studied by infrared spectroscopy: Cooperative and biaxial orientation in semicrystalline polymers. Macromolecules 31(8): 2631–2635
50. Campbell VE, In I, McGee DJ, Woodward N, Caruso A, Gopalan P (2006) Chromophore orientation dynamics, phase stability, and photorefractive effects in branched azobenzene chromophores. Macromolecules 39(3):957–961
51. Kim MJ, Lee JD, Chun C, Kim DY, Higuchi S, Nakayama T (2007) Control of photodynamic motions of azobenzene-derivative polymers by laser excitation wavelength. Macromol Chem Phys 208(16):1753–1763